# Induction of Functional 3D Ciliary Epithelium–Like Structure From Mouse Induced Pluripotent Stem Cells

Hirofumi Kinoshita,[1] Kiyoshi Suzuma,[1] Jun Kaneko,[2] Michiko Mandai,[2] Takashi Kitaoka,[1] and Masayo Takahashi[2]

[1]Department of Ophthalmology and Visual Sciences, Graduate School of Biomedical Sciences, Nagasaki University, Nagasaki, Japan
[2]Laboratory for Retinal Regeneration, Center for Developmental Biology, RIKEN, Kobe, Japan

Correspondence: Kiyoshi Suzuma, Department of Ophthalmology and Visual Sciences, Graduate School of Biomedical Sciences, Nagasaki University, 1-7-1 Sakamoto, Nagasaki 852-8501, Japan; suzuma@nagasaki-u.ac.jp.

Submitted: July 2, 2015
Accepted: December 2, 2015

Citation: Kinoshita H, Suzuma K, Kaneko J, Mandai M, Kitaoka T, Takahashi M. Induction of functional 3D ciliary epithelium–like structure from mouse induced pluripotent stem cells. *Invest Ophthalmol Vis Sci*. 2016;57:153–161. DOI:10.1167/iovs.15-17610

**Purpose.** To generate ciliary epithelium (CE) from mouse induced pluripotent stem (iPS) cells.

**Methods.** Recently, a protocol for self-organizing optic cup morphogenesis in three-dimensional culture was reported, and it was suggested that ocular tissue derived from neural ectoderm could be differentiated. We demonstrated that a CE-like double-layered structure could be induced in simple culture by using a modified Eiraku differentiation protocol.

**Results.** Differentiation of a CE-like double-layered structure could be promoted by glycogen synthase kinase 3β (GSK-3β) inhibitor. Connexin43 and aquaporin1 were expressed in both thin layers, and induced CE-like cells expressed ciliary marker genes, such as *cyclinD2*, *zic1*, *tgfb2*, *aldh1a3*, *wfdc1*, *otx1*, *BMP4*, and *BMP7*. Increases in cytoplasmic and nuclear β-catenin in aggregates of the CE-like double-layered structure were confirmed by Western blot analysis. In addition, tankyrase inhibitor prevented the induction of the CE-like double-layered structure by GSK-3β inhibitor. Dye movement from pigmented cells to nonpigmented cells in the mouse iPS cell–derived CE-like structure was observed in a fluid movement experiment, consistent with the physiological function of CE in vivo.

**Conclusions.** We could differentiate CE from mouse iPS cells in the present study. In the future, we hope that this CE-like complex will become useful as a graft for transplantation therapy in pathologic ocular hypotension due to CE dysfunction, and as a screening tool for the development of drugs for diseases associated with CE function.

Keywords: ciliary epithelium, iPS, GSK-3β, β-catenin

The ciliary body (CB) plays important roles in eye homeostasis. It secretes aqueous humor that maintains IOP, controls the lens shape through the ciliary muscle and ciliary zonules, and synthesizes glycoproteins of the vitreous body. The CB contains a double-layered epithelial structure comprising the inner nonpigmented epithelium (NPE), the outer pigmented epithelium (PE), and the underlying stroma. The NPE is continuous with the neural retina (NR) and the iris pigmented epithelium, while the PE lies between the retinal pigment epithelium (RPE) and the outer iris muscle.[1] The NPE and the PE, as well as the NR and RPE, are derived from neural ectoderm. During eye development, the ciliary epithelium (CE) folds to form the ciliary processes, while neural crest cell–derived stroma cells underneath the CE also contribute to CB morphogenesis.[2] The PE rests on the connective tissue stroma, and the NPE is polarized with its basal lamina facing the posterior chamber of the eye. The PE and NPE interact via their apical membranes with gap junctions.

Water can pass from PE to NPE via gap junctions following NaCl movement[3,4] and exit the NPE to the posterior chamber by using basolaterally located aquaporin (AQP) 1 and/or 4.[5] The IOP is maintained at physiological range by the constant production of aqueous humor from the CB and its outflow through the trabecular meshwork in healthy eyes. Ocular hypertension resulting from a reduced outflow of aqueous humor is a cause of some types of glaucoma in which ganglion cells degenerate. In contrast, ocular hypotension due to reduced fluid production by CB dysfunction caused by ciliochoroidal detachments, severe inflammation, or malignancy can lead to impaired ocular function with loss of vision. So far, there are no treatments for ocular hypotension. If healthy CB could be transplanted and induced to secrete aqueous humor, it could facilitate ocular tension recovery and vision restoration.

Cultured mouse and human embryonic stem (ES) cells can develop into a three-dimensional (3D) optic cup that remarkably resembles the embryonic vertebrate eye.[6,7] With this procedure, we could differentiate mouse induced pluripotent stem (iPS) cells or mouse ES cells into NR, RPE, and tissue derived from the neural ectoderm in the 3D structure. Here, we report the possibility that structured, functional CE could be differentiated from mouse ES/iPS cells.

## Methods

### Animals

All animal experiments were conducted in accordance with the ARVO Statement for the Use of Animals in Ophthalmic and Vision Research and were approved by the RIKEN CDB Animal Experiment Committee (Kobe, Japan). C57BL/6CrSlc mice were purchased from Nihon Slc (Shizuoka, Japan). Animals

TABLE. Primers Used for RT-PCR

| Primers | Sequences |
|---|---|
| CyclinD2 | |
| Forward | CAAAGGAAGGAGGTAAGGGAAGCACTC |
| Reverse | CACGTGAGTGTGTTCACTTCATCATCC |
| Zic1 | |
| Forward | AAAAGTCGTGCAACAAAACTTTCAGCA |
| Reverse | TGCGTGTAGGACTTATCGCACATCTTG |
| Tgfb2 | |
| Forward | AGCACCCTCGACATGGATCAGTTTATG |
| Reverse | AGACCCTGAACTCTGCCTTCACCAGAT |
| Aldh1a3 | |
| Forward | TTCGTCGACCTGGAAGGCTGTATTAAG |
| Reverse | CAAAGCCTGGTACAATGTTCACCACAC |
| Wfdc1 | |
| Forward | AGAAAAGTCCTTCGGGCTCTGAGTTTC |
| Reverse | GCTTAACACACTGTCCATGGTTGGGTA |
| Otx1 | |
| Forward | GCTGTTCGCAAAGACTCGCTACCC |
| Reverse | GAAGCAGTAGGCGTGCTCAGAGAGG |
| BMP4 | |
| Forward | TGCTGATGGTCGTTTTATTATGCCAAG |
| Reverse | GTCCAGTAGTCGTGTGATGAGGTGTCC |
| BMP7 | |
| Forward | ATAAGGACTACATCCGGGAGCGATTTG |
| Reverse | ACCATGAAGGGTTGCTTGTTCTGG |
| G3PDH | |
| Forward | ACCACAGTCCATGCCATCAC |
| Reverse | TCCACCACCCTGTTGCTGTA |

were maintained under standard laboratory conditions (18°C–23°C, 40%–65% humidity, and 12-hour light–dark cycle) with free access to food and water throughout the experimental period.

## Cell Culture

Generation of the *Nrlp*-eGFP transgenic iPS line was described previously.[8] Mouse ES/iPS cells (Rx knock-in GFP ES line mESRx+; *Nrlp*-eGFP transgenic iPS line) were maintained in Glasgow minimum essential medium (GMEM), 10% fetal bovine serum (FBS), 1 mM sodium pyruvate, 0.1 mM nonessential amino acids (NEAA; Invitrogen, Carlsbad, CA, USA), 0.1 mM 2-mercaptoethanol (2-ME), 100 U/mL penicillin and 100 mg/mL streptomycin supplemented with 1000 U/mL leukemia inhibitory factor (LIF), 3 μM CHIR99021, which is a glycogen synthase kinase 3β (GSK-3β) inhibitor, and 1 μM PD0325901, which is a mitogen activated protein kinase kinase (MEK or MAPKK) inhibitor, on gelatin-coated dishes. LIF, CHIR99021, and PD0325901 were freshly added to the culture medium at each medium change. To prepare 4 mL maintenance medium, 4 μL each LIF, CHIR99021, and PD0325901 stock solution were added so that the final concentrations became 1000 U/mL for LIF, 3 μM for CHIR99021, and 1 μM for PD0325901. Special care was taken to avoid overconfluency of mouse ES/iPS cells in maintenance culture, as it might lead to undesirable differentiation of cells. Cells were maintained under feeder-free conditions.

## Retinal Differentiation

Mouse ES/iPS cells were differentiated into NR by serum-free floating culture of embryoid body–like aggregates with quick reaggregation (SFEBq) culture according to the protocol by Eiraku et al.[6] Cells were dissociated into single cells in 0.25% trypsin–ethylenediaminetetraacetic acid (EDTA) and quickly reaggregated in retinal differentiation medium (3000 cells, 100 μL/well) in 96-well low-cell adhesion plates (Lipidure Coat; NOF, Tokyo, Japan). The retinal differentiation medium is GMEM, 1.5% knockout serum replacement (KSR; Invitrogen), 0.1 mM NEAA, 1 mM sodium pyruvate, and 0.1 mM 2-ME. The day on which the SFEBq culture is started is defined as day 0. Matrigel (growth factor-reduced; BD Biosciences, San Jose, CA, USA) was added to the culture medium to a final concentration of 2% on day 1. On day 7, the aggregates were transferred to bacterial-grade plastic dishes and further cultured in suspension in retinal maturation medium 1 (RMM1; Dulbecco's modified Eagle's medium [DMEM], F12 with glutamax, N2 supplement, 100 U/mL penicillin, and 100 mg/mL streptomycin) under 40%-$O_2$/5%-$CO_2$ conditions. After day 10, the aggregates were subjected to suspension culture in retinal maturation medium 2 (RMM2; DMEM, F12 with glutamax, 10% FBS, N2 supplement, 100 U/mL penicillin, and 100 mg/mL streptomycin) supplemented with 0.5 μM all-*trans* retinoic acid (RA) and 1 mM L-taurine for long-term culture.

## Immunohistochemistry

Differentiated tissues were fixed with 4% paraformaldehyde for 10 minutes at 4°C and then permeabilized with 0.3% Triton X-100 for 10 minutes. After 1 hour of blocking with 5% goat serum, cells were incubated with primary antibodies overnight at 4°C and subsequently with secondary antibodies for 1 hour at room temperature. Antibodies against the following proteins were used at the indicated dilutions: AQP1 (rabbit/1:500; Santa Cruz Biotechnology, Santa Cruz, CA, USA), AQP4 (rabbit/1:500; Millipore, Billerica, MA, USA), and Connexin43 (Cx43, rabbit/1:1000; Sigma-Aldrich Corp., St. Louis, MO, USA). 4′,6-diamidino-2-phenylindole (DAPI) was used for counterstaining the nuclei (Molecular Probes, Eugene, OR, USA). Stained sections were analyzed with LSM510 and LSM700 confocal microscopes (Zeiss, Oberkochen, Germany).

## Reverse Transcriptase-Polymerase Chain Reaction (RT-PCR)

Total RNA was extracted from mouse iPS cells in maintenance culture as a control and from differentiated ciliary-like epithelia. The differentiated ciliary-like epithelia, which contained both NPE and PE, were manually excised from the aggregates after day 13. The excision was carefully performed to avoid contamination with unrelated differentiated tissue. Total RNA was extracted with an RNeasy Mini Kit (Qiagen, Valencia, CA, USA) and transcribed with ReverTra Dash (Toyobo, Osaka, Japan), following the manufacturers' instructions. The gene-specific primers used in this research are listed in the Table.

## Western Blot Analysis

Aggregates were washed with PBS and pelleted by centrifugation. For immunoblotting, whole-cell lysates were prepared by using Halt protease and phosphatase inhibitor single-use cocktail (Thermo, Waltham, MA, USA). For nuclear extracts, cells were lysed in NE-PER nuclear and cytoplasmic extraction reagents (Thermo), according to the manufacturer's protocol. Protein concentration was determined by a Bradford assay. Samples were

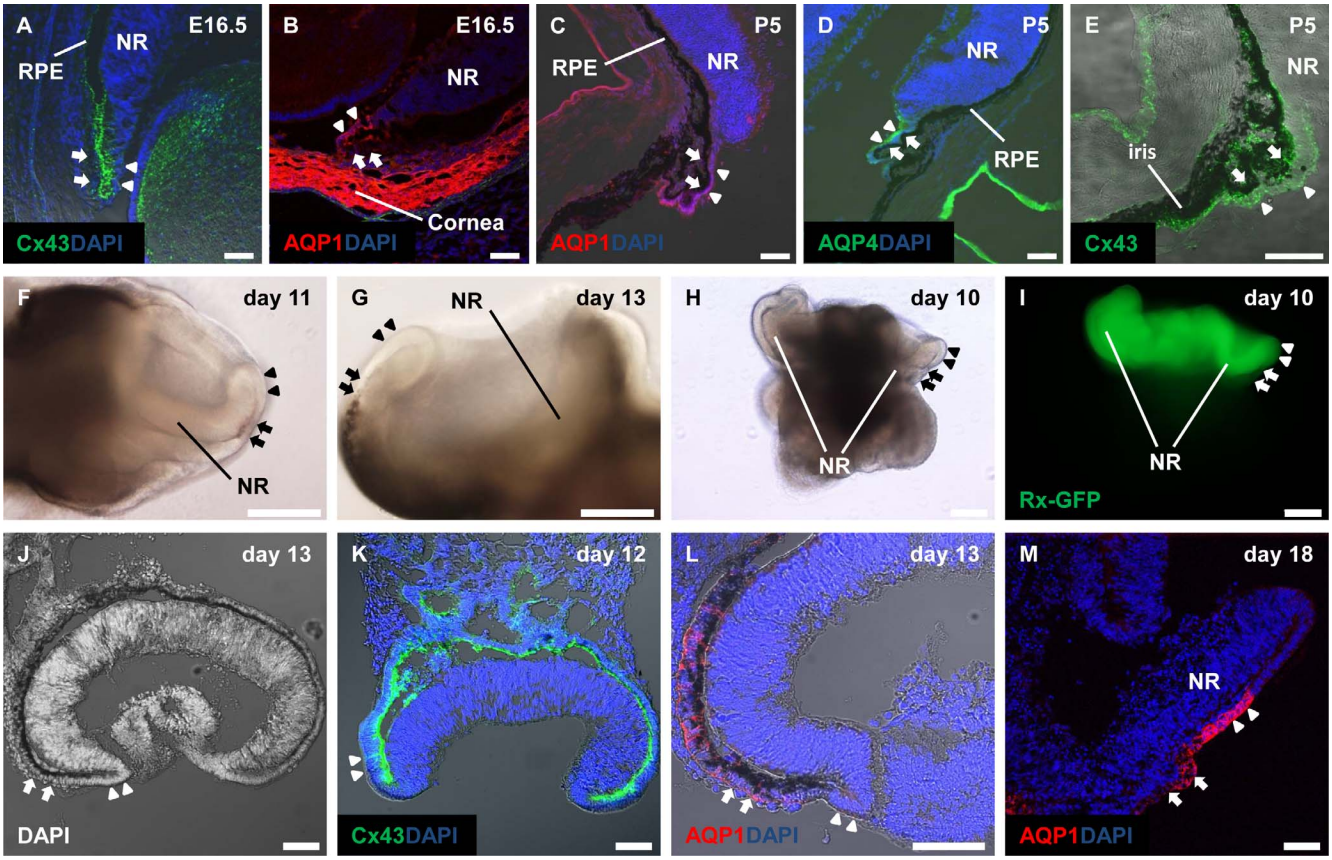


**Figure 1.** Expression of ciliary marker on E16.5 and P5 mouse eye, and 3D culture of mouse iPS and ES cell aggregates. (**A**–**E**) Immunohistochemistry for ciliary marker in E16.5 (**A**, **B**) and P5 (**C**–**E**) C57BL/6J mouse eye. (**A**) Cx43-positive staining is observed in the lens epithelium, CE (NPE and PE), gap junctions between PE (*arrows*) and NPE (*arrowheads*), and RPE. (**B**) AQP1-positive staining is observed in the NPE and cornea. (**C**) AQP1-positive staining is observed in the NPE and iris, especially in the anterior pars plicata. (**D**) AQP4-positive staining is observed in the NPE, especially in the posterior pars plicata. (**E**) Cx43-positive staining is observed in the CE (NPE and PE), gap junction, RPE, and posterior region of the iris. The NPE and PE are opposed to each other. *Scale bars*: 50 μm (**F**–**I**) Optic cup–like structure in 3D culture (Eiraku's protocol) from mouse ES/iPS cells. Optic cup–like structure on day 11 (**F**) and day 13 (**G**) from mouse iPS cells and day 10 (**H**, **I**) from mouse ES cells. (**I**) Optic cup–like structures were positive for Rx-GFP. The NPE-like cells (*arrowheads*) and PE/RPE-like cells (*arrows*) are continuous and not opposed to each other. *Scale bars*: 200 μm. (**J**–**M**) Immunohistochemistry of cryosections of optic cup–like aggregates from mouse iPS cells. (**J**) DAPI-stained nuclei reveal the morphology of optic cup-like aggregates. (**K**) Cx43-positive staining was only observed in the outer layer, and this marker was not expressed at all in the inner layer of the optic cup–like aggregate. (**L**, **M**) AQP1-positive staining was also observed in the outer layer, and similar to Cx43, this marker was not expressed at all in the inner layer of the optic cup–like aggregate. The NPE-like cells (*arrowheads*) and PE/RPE-like cells (*arrows*) are located next to each other. *Scale bars*: 50 μm.

subjected to 10% SDS-PAGE and then analyzed by using a standard Western blotting technique. All primary antibodies for Western blotting were used at a concentration of 1:1000. The following antibodies were obtained from Cell Signaling (Danvers, MA, USA): anti-histone deacetylase 1 (HDAC1), anti-β-actin, and anti-β-catenin (used to confirm equal loading on all blots, with the exception of SDS-PAGE of nuclear extracts where anti-HDAC1 was used to confirm equal loading).

### Fluid Movement Examination of CE-Like Structure

Aggregates examined for fluid movement were cultured on a membrane filter (Millipore) after day 10. The pigmented cell layer (e.g., PE against NPE or RPE against NR) was adhered to the filter side. Then, aggregate with the membrane filter was placed on a glass-bottom dish to be upside-down during the investigation of fluid movement. In other words, it was arranged in the order of membrane filter, PE or RPE, NPE or NR, and glass-bottom dish from above. Lucifer yellow solution was dribbled on the back of the membrane filter, and live imaging of the staining between two layers was observed by z- and time-scan with an LSM700 confocal microscope.

### Statistical Analysis

Statistical analysis was performed with 1-way ANOVA followed by Dunnett's or Tukey's tests. *P* values less than 0.05 were considered statistically significant.

## Results

### The Peripheral Structure of Optic Cup–Like Aggregate From Mouse iPS Cells was Different From That of the Mouse Eye

To evaluate whether the Eiraku retinal differentiation protocol can induce CE, we compared embryonic and postnatal mouse eyes with optic cup–like aggregates derived from mouse ES/iPS cells. As shown in Figures 1A and 1B, CE were seen in the peripheral region of E16.5 mouse eye, and PE (arrows) and NPE (arrowheads) were opposed. In P5 mouse eye, the pars plicata was formed, and NR and CE became more clearly morphologically distinguishable. The opposed arrangement of PE and NPE remained (Figs. 1C–E). Optic cup–like aggregates

derived from mouse ES/iPS cells with Eiraku's protocol also contained NR and RPE (Figs. 1F, 1G), and the optic cup–like aggregates from mouse ES cells were Rx-GFP positive (Figs. 1H, 1I). Rx is a retinal and anterior neural fold homeobox gene that is expressed in the optic vesicle and the optic cup, which are derived from neural ectoderm.[9] Because our tissues derived from mouse ES cells were still in the middle of differentiation, Rx was also expressed in neuroectodermal tissues other than the NR, such as CE. Moreover, the morphology of the peripheral retina was similar to that in vivo, seemingly because the pigmented cells were located in the outer layer, like RPE. However, upon close observation, PE was indistinguishable from RPE, and NPE based on the cell morphology was likely next to PE/RPE continuously located in the outer layer, not in the inner layer in the opposing position of PE like that in vivo (Figs. 1J–M).

For a more detailed examination, we performed immunohistochemistry with Cx43, AQP1, and AQP4, which are expressed on the CE.[5,10] In the mouse eye, Cx43-positive staining was seen in the lens epithelium, RPE and CE, and it was especially evident in the gap junction between PE and NPE (Figs. 1A, 1E). Cx43 immunoreactivity was not seen in the NR. The lens fiber staining was suspected to be nonspecific.[10] AQP1-positive staining was seen in the NPE and iris, especially in the anterior pars plicata (Figs. 1B, 1C). AQP4-positive staining was seen in the NPE, especially in the pars plana (Fig. 1D). In optic cup–like aggregates from mouse ES/iPS cells, there were several differences as compared with the mouse eye. First, AQP1-positive staining was seen in PE/RPE. In previous studies, AQP1 protein was not detected in adult rat or human RPE preparations, possibly because of technical difficulties associated with the presence of melanin and lipofuscin in RPE cells.[11–13] Stamer et al.[14] reported that AQP1 protein was detected in human RPE in situ and in cultures of human adult and fetal RPE cells; the expression of AQP1 by RPE in vivo probably contributes to the efficient transepithelial water transport across RPE, maintains retinal attachment, and prevents subretinal edema. Therefore, AQP1-positive staining in our immature PE/RPE is consistent with previous findings. Second, there was an important difference that, although there were positive regions for ciliary markers, these regions were slightly different from the positive regions in the mouse eye. Cx43- and AQP1-positive staining was seen in the outer layer as we suspected, and these markers were not expressed in the inner layer of optic cup–like aggregates (Figs. 1K–M). Moreover, AQP1-positive staining was also observed in the same outer region on day 18, which is supposedly a more mature state (Fig. 1M). Therefore, it was suggested that the peripheral structure of optic cup–like aggregate from mouse ES/iPS cells did not have original opposed CE structures.

## GSK-3β Inhibitor CHIR99021 Induces Differentiation Into CE

To differentiate structured CE in which NPE and PE are opposed, we tested modified differentiation protocols. With the addition of CHIR99021 (1.2–1.5 μM) from day 7, prospective optic cup–like aggregates formed by Eiraku's protocol started to change into a thin double layer of prospective NPE and PE at day 10 (Figs. 2A–D). This structure was also Rx-GFP positive (Fig. 2B) and took a variety of forms, such as a wing-like form (Fig. 2C) or a cup–like form (Fig. 2D). In the thin double-layered structure, the Cx43 immunoreactivity was observed in the plasma membrane of prospective NPE (arrowheads) and PE (arrows) and the gap junction between the two layers (Fig. 2E). AQP1 was also expressed in both thin layers (Fig. 2F). Also, we investigated the presence of ciliary marker gene messenger RNAs (mRNA)[15–18] in the differentiated CE-like structure excised manually from the aggregates with care to prevent contamination with unrelated differentiated tissue. Induced CE-like cells expressed ciliary marker genes, such as *cyclinD2*, *zic1*, *tgfb2*, *aldh1a3*, *wfdc1*, *otx1*, *BMP4*, and *BMP7*; as expected, mouse iPS cells did not express these ciliary marker genes (Fig. 2G).

## Different CHIR99021 Concentrations Induce Variable Morphologic Changes

Interestingly, variable morphologic changes were observed by treatment with different CHIR99021 concentrations from day 7. Low CHIR99021 concentrations (final concentration, 0.5–1.0 μM) induced structures that were similar to the more original optic cup structure, in that they were composed of not only CE but also NR (Figs. 3A–C, 3E, 3F). Moreover, the expression patterns of Cx43 and AQP1 were also similar to those in vivo (Figs. 3E, 3F). On the other hand, treatment with a high CHIR99021 concentration (final concentration, 3 μM) induced only pigmented cells (Fig. 3D).

## Dye Movement From PE-Like Cells to NPE-Like Cells in CE-Like Structures Derived From Mouse iPS Cells was Observed

To evaluate the function of the induced CE-like structure, we investigated the movement of fluid between the layer of pigmented cells and the layer of nonpigmented cells. Wang et al.[19] showed fluid movement in the CEs by using Lucifer yellow, which passes across gap junctions in dye experiments. For the dye experiment, aggregates were cultured on the membrane filter after day 10, with the pigmented cell layer adhered to the filter side. As described in the Methods, Lucifer yellow solution was dribbled on the back of the membrane filter, and the movement of Lucifer yellow solution between the two layers was observed by z- and time-scan of confocal microscopy (Figs. 4A–C). Optic cup–like aggregates, which have NR- and RPE-like structures and were derived from mouse iPS cells, were used as a control. As shown in Figure 4A, dye movement from pigmented cells (PE-like cells) to nonpigmented cells (NPE-like cells) in CE-like structures derived from mouse iPS cells was observed. However, dye movement from pigmented cells (RPE-like cells) to nonpigmented cells (NR-like cells) was not observed in the controls (Fig. 4B). The direction of fluid movement of PE and RPE derived from mouse iPS cells was different, which is consistent with in vivo observations. These results suggest that epithelia induced from mouse iPS cells play each epithelial role in vivo.

## CE Induced by Stabilized β-Catenin was Blocked by Tankyrase Inhibitor

To evaluate whether differentiation to CE by treatment with CHIR99021 was due to the inhibition of GSK-3β, we used another GSK-3β inhibitor, BIO. In the same way as CHIR99021, treatment with BIO (final concentration, 0.5–1.0 μM) from day 7 induced a CE-like double layer of prospective PE and NPE (Fig. 4D). Next, to confirm whether inhibition of GSK-3β corresponds to canonical Wnt signal activation, we performed Western blot analysis to investigate the β-catenin protein levels in the cytoplasm and nucleus after CHIR99021 treatment (Fig. 4E). In Western blot analysis of CE-like cells, the β-catenin protein levels normalized by β-actin or HDAC1 protein levels were increased in both the cytoplasm and nucleus after 3 hours and later. In cytoplasm, β-catenin levels were significantly increased after 3 hours (2.38 ± 1.05-fold, $P < 0.05$; Dunnett test) and then decreased gradually. In the nucleus, β-

Investigative Ophthalmology & Visual Science

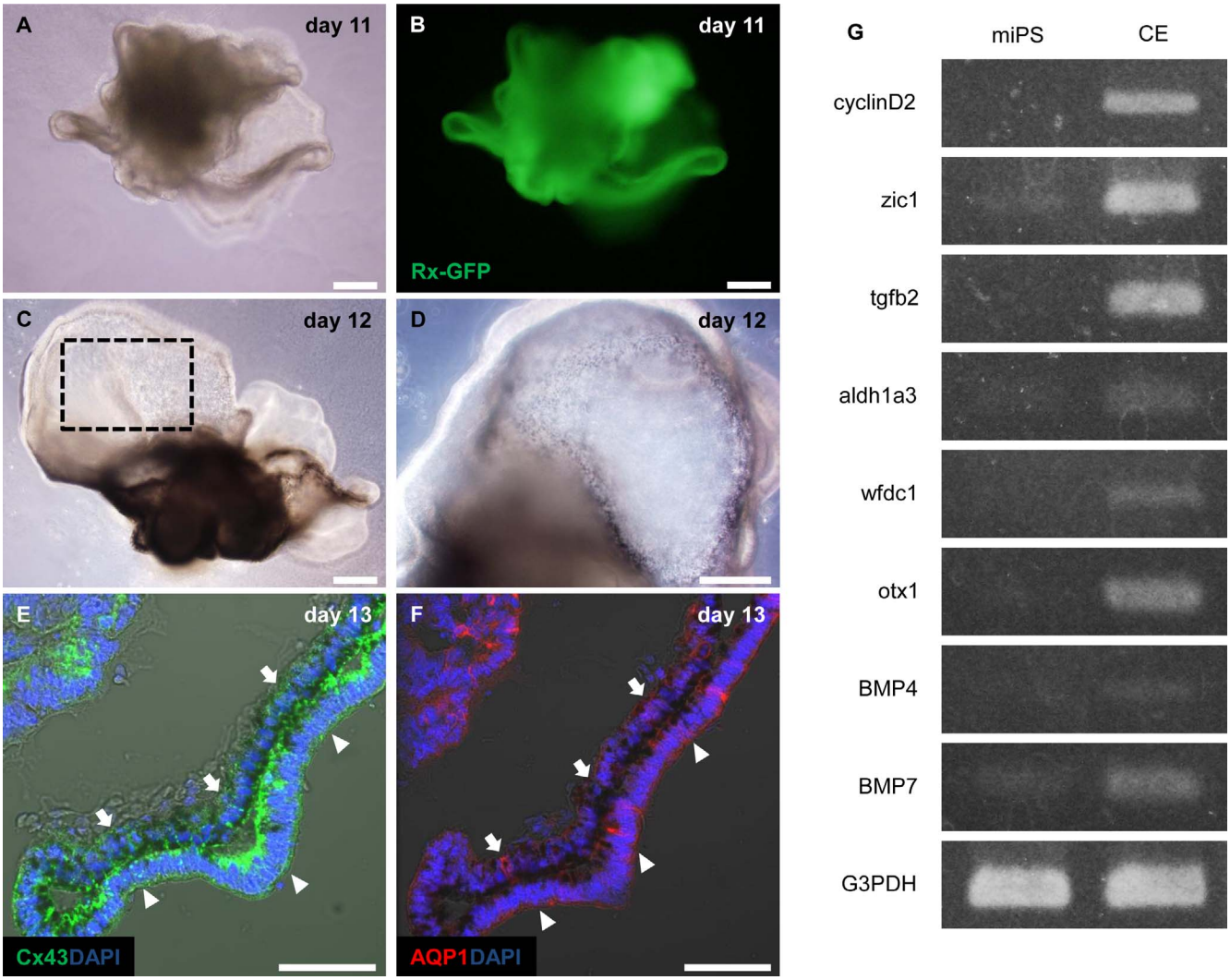


**Figure 2.** Ciliary epithelium–like aggregate from mouse ES/iPS cells. Prospective neural retina of the optic cup–like structure changed into a thin layer structure by the addition of CHIR99021 (1.2–1.5 μM) from day 7; thin double layers of prospective NPE (*arrowheads*) and PE (*arrows*) are formed. (**A**, **B**) Thin double layers on day 11 from mouse ES cells. (**B**) The thin double-layered structure is positive for Rx-GFP. *Scale bars*: 200 μm. (**C**, **D**) Thin double layers of prospective NPE and PE from mouse iPS cells. The whole aggregate changes into CE-like thin double layers by the addition of CHIR99021. Thin double layers take a variety of forms, such as a wing-like form (**C**) or a cup-like form (**D**). *Scale bars*: 200 μm. (**E**, **F**) Immunohistochemistry of thin double-layered structure. Cross-sectional view of a part, such as the blocked area in (**C**). (**E**) Expression of Cx43 was confirmed in the plasma membrane of NPE-like cells (*arrowheads*) and PE-like cells (*arrows*) and in the gap junction between two layers. (**F**) AQP1 was also expressed in both layers. The NPE-like cells and PE-like cells are opposed to each other, and the induced structures are similar to the ciliary double-layered epithelium in vivo. *Scale bars*: 50 μm. (**G**) Comparison of mRNA expression of mouse iPS cells and thin double layer of prospective NPE and PE from mouse iPS cells. G3PDH (GAPDH) is the control.

catenin levels increased significantly after 3 hours (1.76 ± 0.44-fold, $P < 0.01$; Dunnett test) and peaked after 6 hours (2.11 ± 0.84-fold, $P < 0.01$; Dunnett test). These results indicated that β-catenin may participate in differentiation to CE.

Furthermore, to evaluate whether a Wnt signal inhibitor prevents induction to a CE-like thin layer, we tested to see if XAV939 reversed the effect of CHIR99021. XAV939 inhibits tankyrase, which inhibits axin. Therefore, XAV939 inhibits Wnt signal due to axin activation. Treatments of CHIR99021 with or without XAV939 at day 7 were compared (Figs. 4F, 4G). When using XAV939 at day 7, a part of the thin layer became a thick layer at day 10, and Cx43 immunoreactivity was not found in that region (Fig. 4G). Therefore, it was likely that XAV939 inhibits the induction of CE by CHIR99021. Also, β-catenin levels in aggregates after 3 hours of treatment with both CHIR99021 and XAV939 (cytoplasm: 1.77 ± 0.09-fold, nucleus: 1.51 ± 1.11-fold, both not significant) were decreased as compared with CE-like aggregates treated with CHIR99021 only (cytoplasm: 2.53 ± 1.30-fold, nucleus: 1.84 ± 0.77-fold), as determined by Western blot analysis. These results further support the idea that GSK-3β is a key regulator of differentiation to CE. In other words, a canonical Wnt signal, especially stabilized β-catenin, is necessary for induction to the CE double layer.

## Discussion

Several studies have shown that under specifically defined culture conditions, ES and iPS cells can be induced to differentiate along a retinal lineage.[20–26] Recently, milestone work described a 3D embryoid body-based differentiation protocol that mimicked normal development of embryonic

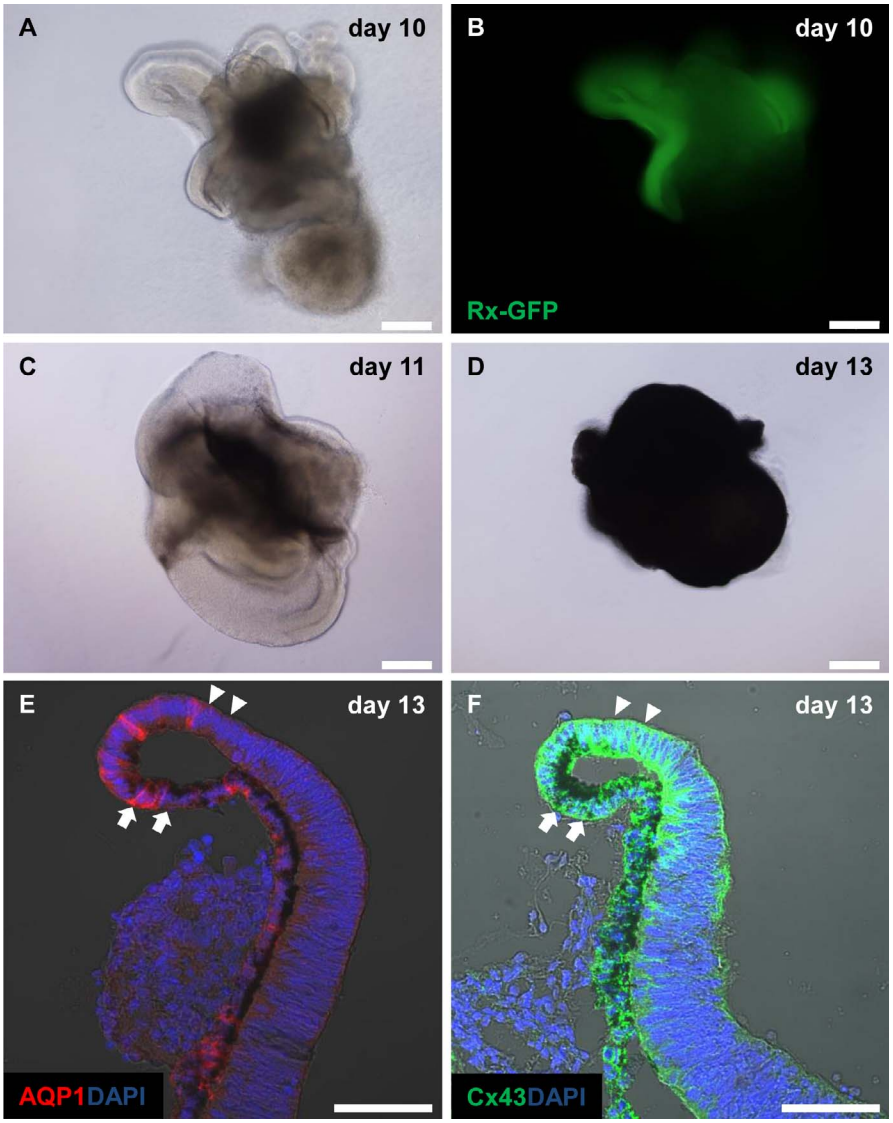


FIGURE 3. Different CHIR99021 concentrations induced variable morphologic changes. (**A**–**C**) CHIR99021 (final concentration, 0.5–1.0 μM) was added to aggregates from day 7. (**A**, **B**) Aggregates on day 10 from mouse ES cells. (**B**) Rx-GFP–positive structure. (**C**) Aggregates on day 11 from mouse iPS cells. *Scale bars*: 200 μm. (**D**) Treatment with a high CHIR99021 concentration (final concentration, 3 μM) induced only pigmented cells. *Scale bars*: 200 μm. (**E**, **F**) Immunohistochemistry of aggregates with added CHIR99021 (final concentration, 0.5–1.0 μM) from mouse iPS cells. Although NR changes into a slightly thin structure, the induced structure is more similar to the peripheral structure of the mouse eye, in that it was composed of not only CE but also NR. The NPE-like cells (*arrowheads*) and PE-like cells (*arrows*) are opposed to each other, and the expression patterns of AQP1 (**E**) and Cx43 (**F**) are also similar in vivo. *Scale bars*: 50 μm.

retinal tissue.[6,7] Several groups have transplanted ES and iPS cell–derived retina produced by 3D culture methods.[27,28] In 2014, another 3D-culture method for retinal tissue from human iPS cells was reported.[29] Moreover, in 2015, an induction method of ciliary marginal zone (CMZ) for the production of high-purity NR tissues was reported by the Sasai lab.[30] The purpose of our present study is induction of the functional CE from mouse ES/iPS cells, the CE is responsible for the secretion of aqueous humor and the transfer of substances and water from the blood in the ciliary stroma into the posterior chamber of the eye. In the CE, water flows from the PE cells via gap junctions into the NPE cells from where the aqueous humor is secreted. Consequently, a proper double-layered alignment of PE and NPE is essential. Therefore, we had to investigate the appropriate conditions for the formation of a paired double layer to generate CE. Here, we have demonstrated the possibility that CE can be induced in simple culture by using a modified Eiraku differentiation protocol that depends on an intrinsic self-organizing program.

Several signaling pathways have been identified in peripheral neural retinal development at the embryonic stage, which consists of the CB and iris. BMP signaling plays an important role in this process.[31] The CB was completely absent in transgenic mice engineered to overexpress Noggin, a BMP antagonist, by using a lens-specific promoter. A model of antiparallel gradients of BMP and fibroblast growth factor (FGF) signals to define the region where the CB can further develop was proposed for chicken retinal development.[32] Wnt2b signaling in the developing optic vesicle and optic cup of chicks induces the CB and iris by losing retinal identity upon Wnt signal activation. This conclusion is supported by the fact that in vivo activation of Wnt signaling in the retina interferes with the maintenance of retinal progenitor identity and leads

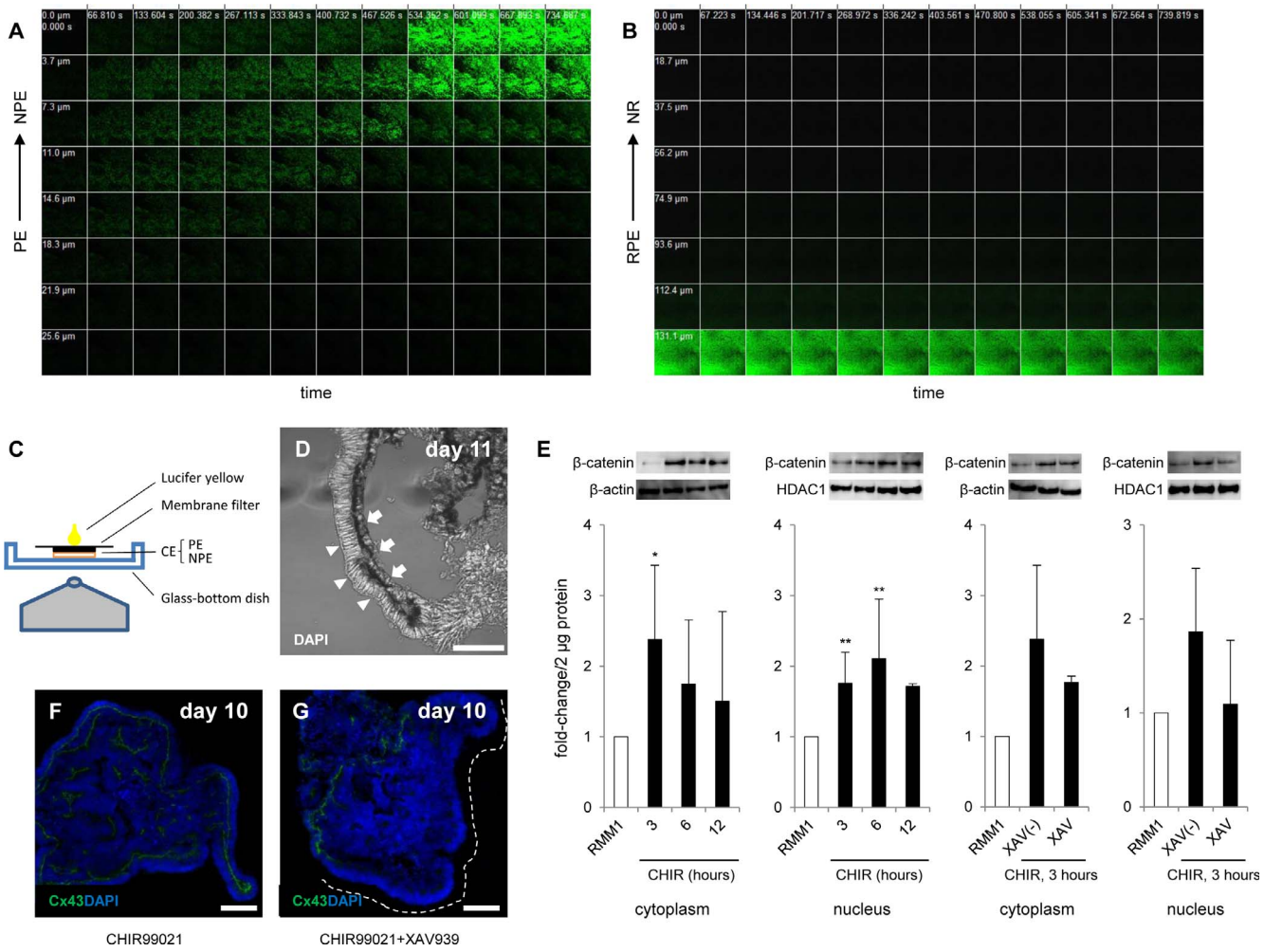


**Figure 4.** Characteristics of CE-like aggregates from mouse iPS cells. (**A**, **B**) Movement of Lucifer yellow solution between two living layers using z- and time-scan of confocal microscopy. The *vertical axis* corresponds to the z-scan, while the *horizontal axis* corresponds to time. Pigmented cells (PE or RPE) correspond to the *bottom* of the figure, and nonpigmented cells (NPE or NR) correspond to the *top* of the figure. (**A**) Ciliary epithelium–like aggregate. Dye movement from pigmented cells to nonpigmented cells was observed. (**B**) Optic cup (NR and RPE)–like aggregate. Dye movement was not observed. (**C**) Schematic diagram of dye experiments. (**D**) Cryosections of aggregate induced by another GSK-3β inhibitor, BIO, from day 7. DAPI-stained nuclei reveal the morphology of the thin double layer of prospective NPE (*arrowheads*) and PE (*arrows*) from mouse iPS cells. *Scale bars*: 50 μm (**E**) Western blot analysis of β-catenin protein levels in the cytoplasm and nucleus of aggregates induced by using CHIR99021. The controls were β-actin for cytoplasm and HDAC1 for the nucleus. The score of β-catenin/control expression was evaluated. After 3 hours, β-catenin protein levels in the cytoplasm and nucleus of CE-like aggregates were increased. In cytoplasm, β-catenin protein levels after 3 hours increased significantly and then decreased gradually. In the nucleus, β-catenin levels after 3 hours increased significantly and peaked after 6 hours. After 3 hours, β-catenin protein levels of aggregates treated by both CHIR99021 and XAV939 decreased as compared with CE-like aggregates treated by CHIR99021 only. (**F**, **G**) Cryosections of aggregate induced by CHIR99021 with or without XAV939 reagent. (**G**) By using XAV939 at day 7, a part of the thin layer became a thick layer at day 10. Positive staining of Cx43 was not identified in that region by immunohistochemistry (*white dotted line*). *Scale bars*: 100 μm.

to the conversion of retinal cells into the peripheral fates of CB and iris. Cho and Cepko[33] also reported that the expression of Wnt2b or constitutively active β-catenin inhibited retinal progenitor gene expression and the differentiation of retinal neurons, and Wnt signal activation in the central retina was sufficient to induce the expression of markers of the CB and iris, two tissues derived from the peripheral optic cup. The same conclusion that activation of canonical Wnt signaling is sufficient and necessary for the normal development of anterior eye structures was reached.[34] Based on these previous reports, we added CHIR99021, which was used for maintenance of undifferentiated mouse ES/iPS cells in our experiments, into retinal differentiation medium because GSK-3β inhibitor has a function equivalent to the activation of the canonical Wnt signal. Fortunately, adding the appropriate concentration (final concentration, 1.2–1.5 μM) of CHIR99021 at the optic vesicle stage induced noteworthy structural change. As shown in the Results, induced structures had double layers consisting of pigmented cells and nonpigmented cells. Moreover, several protein and mRNA markers for CE were confirmed (Fig. 2).

Another GSK-3β inhibitor could also induce the formation of thin CE-like double layers. Activation of the canonical Wnt pathway results in the stabilization and accumulation of cytoplasmic β-catenin, which is otherwise phosphorylated in a protein complex containing GSK-3β and targeted for degradation. Stabilized β-catenin translocates to the nucleus and associates with TCF/Lef (T-cell–specific transcription factor and lymphoid enhancer-binding factor) transcription factors and other cofactors to activate target gene transcrip-

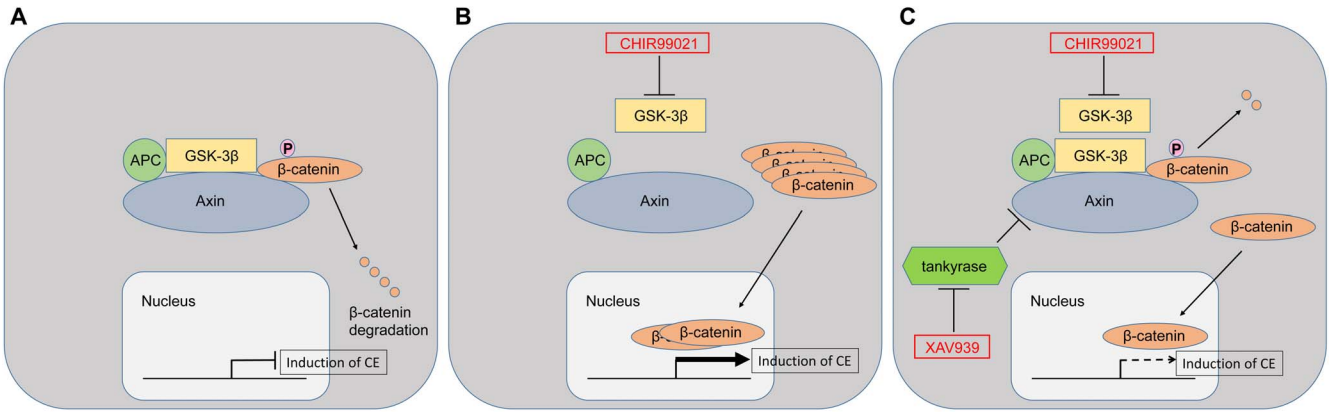


**Figure 5.** Mechanism of induction to CE-like aggregate from mouse iPS cells. (**A**) β-catenin forms a complex with axin, adenomatous polyposis coli, and GSK-3β, and it is degraded by the ubiquitin-proteasome system. (**B**) Glycogen synthase kinase 3β is inactivated via GSK-3β inhibitor, CHIR99021, or BIO. Cytoplasmic β-catenin is stabilized, and the accumulated β-catenin is translocated into the nucleus. Stabilized β-catenin promotes the induction of CE (**C**) Axin is relatively activated due to inhibition of tankyrase by XAV939. Therefore, degradation of β-catenin may be relatively increased as compared with when only GSK-3β inhibitor is administered. A decreased level of β-catenin translocated into the nucleus does not promote the induction of CE-like double layers. APC, adenomatous polyposis coli.

tion.[35,36] Therefore, we examined β-catenin expression. Increases in cytoplasmic and nuclear β-catenin were confirmed by Western blot analysis (Fig. 4E). In addition, XAV939 prevented the induction of CE-like double layers by adding CHIR99021. Based on these results, it was suggested that activation of the canonical Wnt signal by translocation of β-catenin to the nucleus has an important role to induce the generation of CE (Fig. 5).

There is considerable controversy with respect to the neurogenic and proliferative effects of the canonical Wnt pathway in the retina. In *Xenopus*, activation of this pathway is required for retinal neurogenesis,[37] whereas in the chick and mouse retina it inhibits neurogenesis[33,34,38–41] and neuronal differentiation.[42] Increased Wnt signaling in the chick eye at the optic vesicle stage, either through expression of cWnt2b, a canonical Wnt ligand, or constitutively active β-catenin, inhibits neuronal differentiation and promotes the development of peripheral eye structures including the CMZ, CB, and iris.[33,34,39,40] Consistent with these previous reports, the concentration gradient of stabilized β-catenin induced ocular tissue derived from neural ectoderm in the present study. In the neural ectoderm region at the optic vesicle, GSK-3β inhibitor could change the fate of tissues such as NR, RPE, or CE. None of the CHIR99021 concentrations added in the optic cup stage could induce morphologic change. Additionally, CE-like double layers could not be maintained in a more mature state, such as on day 20, even when CHIR99021 was continuously added. Therefore, these results suggest that the timing of the induced signal is important, and we speculate that other signals such as BMP and FGF are each individually or interactively needed for more mature development, although GSK-3β inhibitor influences the start of CE induction.

In evaluating CB function, we examined aqueous humor production as its most important role. As shown in the results, fluid movement from PE to NPE in the CE-like aggregates was different from that in the controls, which were optic cup–like aggregates. It seemed that each aggregate induced from mouse iPS cells is consistent with each physiological direction of fluid movement in vivo, such as from PE to NPE and from NR to RPE. Therefore, our induced CE-like structure is totally consistent with "in vivo CE."

Chronic hypotony can progress to a desperate state of phthisis bulbi, although many eyes can still stabilize in a prephthisical state with a low but measurable IOP ranging from 0 to 5 mm Hg. A previous study has reported that inadequate aqueous production could be caused by ciliochoroidal detachments, disruption of the NPE, inflammation, atrophy or loss of CE, and vascular compromise.[43] Therefore, the production and use of new CE could lead to improvement of abnormal ciliary function, prevention of phthisis bulbi, and recovery of visual acuity. Future research should focus on the creation of an adequate form and size of CE from human ES or iPS cells. Additionally, it may be interesting to investigate how the characteristic morphology of the CB, such as pars plicata, is induced, and what signals or physical stimulation are required.

We could differentiate functional CE from mouse ES/iPS cells in the present study. We believe that our results will potentially contribute to the development of a transplantation therapy for noncurable ocular hypotony and to a drug development that may affect aqueous production.

## Acknowledgments

The authors thank the members of the Takahashi Lab and Sasai Lab in RIKEN for their helpful discussions and comments on the experiments.

Disclosure: **H. Kinoshita**, None; **K. Suzuma**, None; **J. Kaneko**, None; **M. Mandai**, None; **T. Kitaoka**, None; **M. Takahashi**, None

## References

1. Beebe DC. Development of the ciliary body: a brief review. *Trans Ophthalmol Soc U K*. 1986;105:123–130.
2. Johnston MC, Noden DM, Hazelton RD, Coulombre JL, Coulombre AJ. Origins of avian ocular and periocular tissues. *Exp Eye Res*. 1979;29:27–43.
3. Civan MM, Macknight AD. The ins and outs of aqueous humour secretion. *Exp Eye Res*. 2004;78:625–631.
4. McLaughlin CW, Peart D, Purves RD, Carre DA, Macknight AD, Civan MM. Effects of HCO3– on cell composition of rabbit ciliary epithelium: a new model for aqueous humor secretion. *Invest Ophthalmol Vis Sci*. 1998;39:1631–1641.
5. Yamaguchi Y, Watanabe T, Hirakata A, Hida T. Localization and ontogeny of aquaporin-1 and -4 expression in iris and ciliary epithelial cells in rats. *Cell Tissue Res*. 2006;325:101–109.
6. Eiraku M, Takata N, Ishibashi H, et al. Self-organizing optic-cup morphogenesis in three-dimensional culture. *Nature*. 2011; 472:51–56.

7. Nakano T, Ando S, Takata N, et al. Self-formation of optic cups and storable stratified neural retina from human ESCs. *Cell Stem Cell*. 2012;10:771–785.
8. Homma K, Okamoto S, Mandai M, et al. Developing rods transplanted into the degenerating retina of Crx-knockout mice exhibit neural activity similar to native photoreceptors. *Stem Cells*. 2013;31:1149–1159.
9. Furukawa T, Kozak CA, Cepko CL. Rax, a novel paired-type homeobox gene, shows expression in the anterior neural fold and developing retina. *Proc Natl Acad Sci U S A*. 1997;94:3088–3093.
10. Calera MR, Topley HL, Liao Y, Duling BR, Paul DL, Goodenough DA. Connexin43 is required for production of the aqueous humor in the murine eye. *J Cell Sci*. 2006;119:4510–4519.
11. Nielsen S, Smith BL, Christensen EI, Agre P. Distribution of the aquaporin CHIP in secretory and resorptive epithelia and capillary endothelia. *Proc Natl Acad Sci U S A*. 1993;90:7275–7279.
12. Stamer WD, Snyder RW, Smith BL, Agre P, Regan JW. Localization of aquaporin CHIP in the human eye: implications in the pathogenesis of glaucoma and other disorders of ocular fluid balance. *Invest Ophthalmol Vis Sci*. 1994;35:3867–3872.
13. Hamann S, Zeuthen T, La Cour M, et al. Aquaporins in complex tissues: distribution of aquaporins 1-5 in human and rat eye. *Am J Physiol*. 1998;274:C1332–C1345.
14. Stamer WD, Bok D, Hu J, Jaffe GJ, McKay BS. Aquaporin-1 channels in human retinal pigment epithelium: role in transepithelial water movement. *Invest Ophthalmol Vis Sci*. 2003;44:2803–2808.
15. Diehn JJ, Diehn M, Marmor MF, Brown PO. Differential gene expression in anatomical compartments of the human eye. *Genome Biol*. 2005;6:R74.
16. Escribano J, Coca-Prados M. Bioinformatics and reanalysis of subtracted expressed sequence tags from the human ciliary body: identification of novel biological functions. *Mol Vis*. 2002;8:315–332.
17. Kubota R, McGuire C, Dierks B, Reh TA. Identification of ciliary epithelial-specific genes using subtractive libraries and cDNA arrays in the avian eye. *Dev Dyn*. 2004;229:529–540.
18. Thut CJ, Rountree RB, Hwa M, Kingsley DM. A large-scale in situ screen provides molecular evidence for the induction of eye anterior segment structures by the developing lens. *Dev Biol*. 2001;231:63–76.
19. Wang Z, Do CW, Valiunas V, et al. Regulation of gap junction coupling in bovine ciliary epithelium. *Am J Physiol Cell Physiol*. 2010;298:C798–C806.
20. Hirami Y, Osakada F, Takahashi K, et al. Generation of retinal cells from mouse and human induced pluripotent stem cells. *Neurosci Lett*. 2009;458:126–131.
21. Ikeda H, Osakada F, Watanabe K, et al. Generation of Rx+/Pax6+ neural retinal precursors from embryonic stem cells. *Proc Natl Acad Sci U S A*. 2005;102:11331–11336.
22. Kamao H, Mandai M, Okamoto S, et al. Characterization of human induced pluripotent stem cell-derived retinal pigment epithelium cell sheets aiming for clinical application. *Stem Cell Rep*. 2014;2:205–218.
23. Lamba DA, Karl MO, Ware CB, Reh TA. Efficient generation of retinal progenitor cells from human embryonic stem cells. *Proc Natl Acad Sci U S A*. 2006;103:12769–12774.
24. Meyer JS, Shearer RL, Capowski EE, et al. Modeling early retinal development with human embryonic and induced pluripotent stem cells. *Proc Natl Acad Sci U S A*. 2009;106:16698–16703.
25. Osakada F, Ikeda H, Mandai M, et al. Toward the generation of rod and cone photoreceptors from mouse, monkey and human embryonic stem cells. *Nat Biotechnol*. 2008;26:215–224.
26. Tucker BA, Park IH, Qi SD, et al. Transplantation of adult mouse iPS cell-derived photoreceptor precursors restores retinal structure and function in degenerative mice. *PLoS One*. 2011;6:e18992.
27. Assawachananont J, Mandai M, Okamoto S, et al. Transplantation of embryonic and induced pluripotent stem cell-derived 3D retinal sheets into retinal degenerative mice. *Stem Cell Rep*. 2014;2:662–674.
28. Gonzalez-Cordero A, West EL, Pearson RA, et al. Photoreceptor precursors derived from three-dimensional embryonic stem cell cultures integrate and mature within adult degenerate retina. *Nat Biotechnol*. 2013;31:741–747.
29. Zhong X, Gutierrez C, Xue T, et al. Generation of three-dimensional retinal tissue with functional photoreceptors from human iPSCs. *Nat Commun*. 2014;5:4047.
30. Kuwahara A, Ozone C, Nakano T, Saito K, Eiraku M, Sasai Y. Generation of a ciliary margin-like stem cell niche from self-organizing human retinal tissue. *Nat Commun*. 2015;6:6286.
31. Zhao S, Chen Q, Hung FC, Overbeek PA. BMP signaling is required for development of the ciliary body. *Development*. 2002;129:4435–4442.
32. Dias da Silva MR, Tiffin N, Mima T, Mikawa T, Hyer J. FGF-mediated induction of ciliary body tissue in the chick eye. *Dev Biol*. 2007;304:272–285.
33. Cho SH, Cepko CL. Wnt2b/beta-catenin-mediated canonical Wnt signaling determines the peripheral fates of the chick eye. *Development*. 2006;133:3167–3177.
34. Liu H, Xu S, Wang Y, et al. Ciliary margin transdifferentiation from neural retina is controlled by canonical Wnt signaling. *Dev Biol*. 2007;308:54–67.
35. Brembeck FH, Rosario M, Birchmeier W. Balancing cell adhesion and Wnt signaling, the key role of beta-catenin. *Curr Opin Genet Dev*. 2006;16:51–59.
36. Widelitz R. Wnt signaling through canonical and non-canonical pathways: recent progress. *Growth Factors*. 2005;23:111–116.
37. Van Raay TJ, Moore KB, Iordanova I, et al. Frizzled 5 signaling governs the neural potential of progenitors in the developing Xenopus retina. *Neuron*. 2005;46:23–36.
38. Fu X, Sun H, Klein WH, Mu X. Beta-catenin is essential for lamination but not neurogenesis in mouse retinal development. *Dev Biol*. 2006;299:424–437.
39. Heavner WE, Andoniadou CL, Pevny LH. Establishment of the neurogenic boundary of the mouse retina requires cooperation of SOX2 and WNT signaling. *Neural Dev*. 2014;9:27.
40. Kubo F, Takeichi M, Nakagawa S. Wnt2b controls retinal cell differentiation at the ciliary marginal zone. *Development*. 2003;130:587–598.
41. Nakagawa S, Takada S, Takada R, Takeichi M. Identification of the laminar-inducing factor: Wnt-signal from the anterior rim induces correct laminar formation of the neural retina in vitro. *Dev Biol*. 2003;260:414–425.
42. Ouchi Y, Tabata Y, Arai K, Watanabe S. Negative regulation of retinal-neurite extension by beta-catenin signaling pathway. *J Cell Sci*. 2005;118:4473–4483.
43. Coleman DJ. Evaluation of ciliary body detachment in hypotony. *Retina*. 1995;15:312–318.


Investigative Ophthalmology & Visual Science